Jordan Journal of Pharmaceutical Sciences, Volume 14, No. 3, 2021

Development of a novel filtered-based pharmacophore for the identification of human equilibrative nucleoside transporter 1 inhibitors

Azza Ramadan,[1,] Shaima Hasan,[1] Sedra Jamal,[1] Ismail Moumen,[1] Noor Atatreh,[1] and Mohammad A Ghattas*[1]*

[1] College of Pharmacy, Al Ain University, Abu Dhabi, United Arab Emirates
* These authors made equal contributions, joint 1st-authorship
Correspondence
* Mohammad A Ghattas, College of Pharmacy, Al Ain University, Abu Dhabi, United Arab Emirates.

ABSTRACT

The human equilibrative nucleoside transporters (hENTs) are important proteins that allow nucleosides and nucleobases permeation into the cell. hENT 1 is a promising target against heart and Huntington's diseases as its inhibition mediates cardiac- and neural protection effects, respectively. However, the current hENT1 inhibitors have significant off-target effects and poor pharmacological profile, hence there is need for new novel inhibitors. Therefore, we developed a computational protocol that identified and selected inhibitors of hENT1 in an efficient and specific manner. First, several pharmacophores were created using a set of known inhibitors. Consequently, the best inhibitor pharmacophore exhibited as high selectivity and specificity rates as 92% and 88%, respectively. Furthermore, another pharmacophore was validated for the oppositely acting type of the hENT1 molecules (i.e. permeants) to act as an extra refinement step in our search for hENT1 inhibitors. Interestingly, employing the inhibitor pharmacophore as a filter-in along with the permeant pharmacophore as a filter-out resulted in up to two-fold enhancement of docking-based virtual screening results of hENT1 inhibitors. This in silico approach can prove very useful in the development of new cardio- and neuroprotective hENT1 inhibitors.

Keywords: Drug design, human equilibrative nucleoside transporter 1, inhibitor, permeant, pharmacophore.

INTRODUCTION

Equilibrative nucleoside transporters (ENTs) are transmembrane integral membrane proteins responsible for the transport of nucleosides and nucleobases across membranes of cells. Purine and pyrimidine nucleosides and nucleobases are crucial biological molecules for prokaryotic and eukaryotic cell physiology as they are the building blocks for DNA/RNA synthesis.[1,2] Certain cell types such as the brain and bone marrow cells are incapable of nucleotides *de novo* synthesis. Hence, they rely solely on the ENT salvage pathway for their nucleobase/nucleoside requirements. Moreover, ENTs regulate the flux of nucleosides such as adenosine across the cell membrane and therefore indirectly influence the purinergic cell singling pathway.[1-3] ENTs role is not limited to its physiological contribution but pharmacologically, ENTs are primary drug targets shown to modulate the efficacy of > 30 FDA/EMA approved drugs, including cardiovascular agents.[1] ENTs serve as a molecular target for drug binding, such as antihypertensive and antiarrhythmic agents,[1] that mediates their cardioprotective effects.

To date, four human ENTs isoforms (hENT1-4) have

Received on 19/1/2021 and Accepted for Publication on 6/6/2021.

been identified with hENT1 being the most studied and best characterized.[1,4] hENT1 is ubiquitously distributed and primarily found in the plasma membranes of various tissues [1,2,5]. The structure of hENT1 consists of 11 TM helices with extracellular C-terminus and cytoplasmic N-terminus.[1,6] The structure was confirmed by glycosylation scanning mutagenesis[7] and more recently by the first crystal structure of this protein.[8] Crystallography structural studies of the inhibitors nitrobenzylthioinosine (NBTI) and dilazep-hENT1 complexes show that these two inhibitors shared a binding site termed "orthosteric site" within the hENT1 central cavity.[8] Potent hENT1 inhibitors include the adenosine analog, NBTI, and coronary vasodilators, dipyridamole and dilazep, with K_i values reported to be in the nanomolar range.[2] Furthermore, hENT1 is inhibited by a vast array of structurally diverse agents such as tyrosine- and serine/threonine kinase inhibitors, benzodiazepines, and calcium channel blockers but to a lesser extent than the aforementioned potent inhibitors.[1,2]

Therapeutically, hENT1 is a target for drugs that are inhibitors which blocks its transport activity. ENT1 inhibitor's therapeutic role in ischemic heart disease and cardioprotection has been well established. ENT1 genetic knockout or pharmacological inhibition via NBTI and dipyridamole resulted in attenuation of myocardial damage evident by the reduction in infarct size and ventricular dysfunction following ischemia/perfusion injury.[9-12] The nucleoside adenosine mediates ENT1 cardioprotective effect. ENT1 inhibition increase adenosine extracellular concentration, which potentiates adenosine receptors-purinergic signaling cardioprotective effects.[2,12,13]

Several lines of evidences have shown that ENT1 inhibition and enhanced adenosine mediated signaling has a neuroprotective effect. Prior research has shown that ENT1 was upregulated in Huntington's disease mouse models and patients at the early severity stage.[14,15] Moreover, extracellular striatal level of adenosine was significantly lowered in two Huntington's disease mouse models than controls,[14] potentially due to enhanced intracellular uptake of adenosine via the upregulated ENT1. It was established that ENT1 pharmacological inhibition via JMF1907 or ENT1 genetic removal increased striatum extracellular adenosine and enhanced survival of Huntington's diseased mice.[15] Furthermore, N6-(4-hydroxybenzyl) adenine riboside (designated T1-11), an adenosine receptor A2AR activator and ENT1 inhibitor, was shown to reduce deterioration of motor coordination and striatal Htt aggregates, a major pathological feature of Huntington's disease.[16] Hence, ENT1 inhibitors can serve as a promising therapeutic target for delaying the onset and treatment of Huntington's disease.[14,17]

Despite the therapeutic application of hENT1 inhibitors, limitations/unfavourable pharmacological properties associated with the present potent inhibitors has been reported. NBTI off-target effects have been reported in the cardiovascular system.[18] and the nitro group of NBTI has been suggested to cause potential liver toxicity.[18] Furthermore, it has been suggested that the polar nature of NBTI reduces its oral bioavailability and crossing through the blood-brain barrier.[19] Dipyridamole has a high binding affinity for α1-acid glycoprotein, which lowers its availability and efficacy as a nucleoside transporter inhibitor.[18] **Given the significant limitations of the current hENT1 inhibitors,** there is an imperative need to develop new hENT1 inhibitors. In this project, we aim to develop a computational approach that can efficiently identify the therapeutically valuable hENT1 inhibitors by investigating their physicochemical characteristics and establishing their pharmacophoric features. The data extracted from this step will be then employed in a novel structure-based drug discovery approach.

2. METHODS

2.1 Pharmacophore generation

As a starting point for developing the pharmacophore model, the inhibitor database underwent ligand preparation by Maestro software using LigPrep where accurate, energy minimized 3D structure for each ligand with all tautomeric and ionization states (at pH 7.4 ± 0.2, i.e., physiological pH) were generated. Additionally, ring conformations, and

stereoisomerism were taken into consideration at this stage to ensure the generation of each molecule's biologically active form in the inhibitors dataset.

For the pharmacophore generation, the pharmacophore features (queries) are constructed based on ligands superimposed conformations (aligned on top of each other) in MOE software to determine features that are common to the aligned ligands.[20] Initially, a "training set" was prepared for the inhibitor's library based on several selection criteria such as the number of rotatable bonds, molecular weight, various structural scaffolds, and IC_{50}/ K_i values.

2.2 Docking into the hENT1 transporter

For docking, co-crystallized structure for the hENT1 transporter with an inhibitor was obtained from the protein data bank (PDB, ID: 6OB7)[8]. The co-crystallized inhibitor and the water molecules were removed from the hENT1 structure. The removal of water was considered in this case as we do not have enough data about the presence of highly structured waters in the active site that are usually considered during docking.[21]

The protein structure preparation was then carried out by MOE using the protein preparation wizard that checks for missing residues, atoms, or loops and makes the corrections accordingly.[22] Later, H-bond optimization for the protein was performed by Protonate 3D method to maximize H-bond networks and reduce the overall self-energy. Further protein preparation was performed by the Maestro protein preparation module prior to Grid generation.[23] Using Receptor Grid Generation in Glide, a grid box was created to contain the docking site. The ligand-binding site was considered a centroid for grid box generation, consisting of a three-dimensional network of regularly spaced points. For all VS protocols, the ligands were docked into the hENT1 binding site using the Glide docking tool in Maestro using the GLIDE-XP method.[24]

3.3 Analysis of hENT1–Inhibitor complexes

The protein-ligand interaction fingerprint (PLIF) method has been previously described.[25] The generated PLIF graph showed the interaction occupancy of all residues present within the hENT1 binding site.

3. RESULTS AND DISCUSSUION

3.1 hENT1 inhibitors database building

The first step of the study was the development of the hENT1 inhibitors library to determine their general structural characteristics and pharmacophoric features. An extensive search of the literature was performed to compile a library of known hENT1 inhibitors along with their K_i/IC_{50} values. Using various search engines, a set of 56 known inhibitors were identified from the literature mining (Supporting Information Table S1, S2). For comparative analysis, we also prepared an additional library that constitutes of 18 known hENT1 permeants (Supporting Information Table S3, S4), which are substrates that are transported intracellularly via hENT1.[1] Then, a 3D structures of all ligands were built and prepared, via the MOE software[26] resulting in two databases, one that contained the inhibitors molecules, while the other one contained the permeants.

3.2 Physiochemical properties assessment

To determine the general structural characteristics of the inhibitors, several physicochemical properties were computationally calculated using the MOE descriptors calculator function[27] and compared to the permeant's physicochemical properties (Table 1). It was observed that the mean molecular weight (mean MWT) for inhibitors was 473.52 Da, which was 76% larger than permeants (269.7 Da). Also, inhibitors seemed to be much more flexible than permeants, as they had a greater number of rotatable bonds by more than four-fold, with a mean value of 10 in comparison to 2.22 in permeants. In terms of polarity, inhibitors showed higher hydrophobicity than permeants as they exhibited a higher value of partition coefficient and hydrophobic surface area (Log P 1.87, HSA 708.63 Å2) than that of permeants (Log P: -1.56, HSA: 423.79). Furthermore, hydrogen bonding capability was less in inhibitors than in permeants as the mean number of hydrogen bond acceptors for inhibitors and permeants was 4.82 and 6.05, respectively, while the mean

number of hydrogen bond donors was 2.0 and 3.72, respectively. Hence, in terms of binding, the inhibitors are more likely to bind through hydrophobic contact. To sum up, while permeants seem to occupy small hydrophilic pocket, the hENT1 inhibitors appear to sit in a larger pocket (that might be partially shared with permeants), with the ability to make a mixed type of polar and nonpolar contacts with the surrounding residues.

3.3 Pharmacophore hENT1 inhibitor model generation

Four molecules from different scaffolds, that were small in size, least flexible and had different levels of K_i/IC_{50} values, were chosen as the training set for the hENT1 inhibitor pharmacophore generation (i.e., NBTI, Dipyridamole, Diazepam, and Dimoxyline) (Figure 1, Supporting information Table S1)

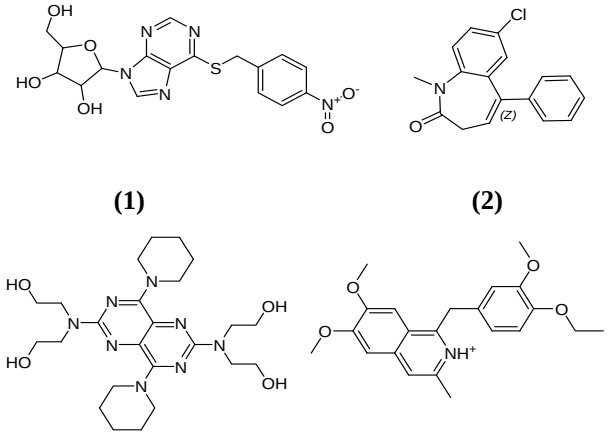

(1) **(2)**

(3) **(4)**

Figure 1. Structures of inhibitor's training set. (1) NBTI, (2) Diazepam, (3) Dipyridamole, (4) Dimoxyline.

The hENT1 inhibitors training set was then used to generate the pharmacophore models using the MOE software pharmacophore elucidator. The objective of pharmacophore elucidation is to search for the pharmacophore queries (denoted as PH4) with the best overlay of the superimposed conformations of the training set.[26,28] Also, we specified seven pharmacophore features which were Hydrogen bond donor/acceptor (Don/Acc), Aromatic (Aro), Hydrophobic (Hyd), Hydrogen bond donor/acceptor projection (Don2/ Acc2), Pi ring (PiR), cationic (Cat) and anionic (Ani) to be taken into account when generating the pharmacophore queries (Supporting information Table S5). This step resulted in the generation of many queries, from which the top 50 with the highest overlaying score were selected. These pharmacophore queries were then validated using a "test set" of known hENT1 ligands, which were either inhibitors or permeants (Supporting information, Table S2, S4). These inhibitors and permeants test sets were used in assessing the selectivity (Se) and specificity (Sp) rates of the pharmacophore queries. Selectivity assesses the efficiency of the developed pharmacophores in selecting the desired ligand (true positives), while specificity measures the pharmacophore efficiency in eliminating those ligands that belong to the other class of hENT1 ligand (which were added as true negatives in this case). [29]

A four- and five- feature pharmacophore queries were generated from the training set's four inhibitors. Table 2 lists the top pharmacophoric queries with the best selectivity and specificity rates. Although PH4-40 had the highest specificity value of 100% among other pharmacophores, it couldn't pick up more than 90% of the

inhibitors compared to those that picked 92.3% and 94.23% of the screened inhibitors as seen in PH4-36 and PH4-4. The pharmacophore PH4-36 showed the best balance of selectivity and specificity, with Se and Sp values of 92.3% and 87.5%, respectively (Table 2). This means that PH4-36 was able to pick more than 90% of the screened inhibitors while filtering out more than 80% of the screened permeants. Figure 2a shows the most active hit inhibitor aligned to PH4-36, fulfilling all pharmacophore features. On the other hand, Figure 2b shows one of the filtered-out permeant along with PH4-36 that did not fulfil the pharmacophore where the two hydrophobic features were absent, as well as the absence of H-bond acceptor projection feature.

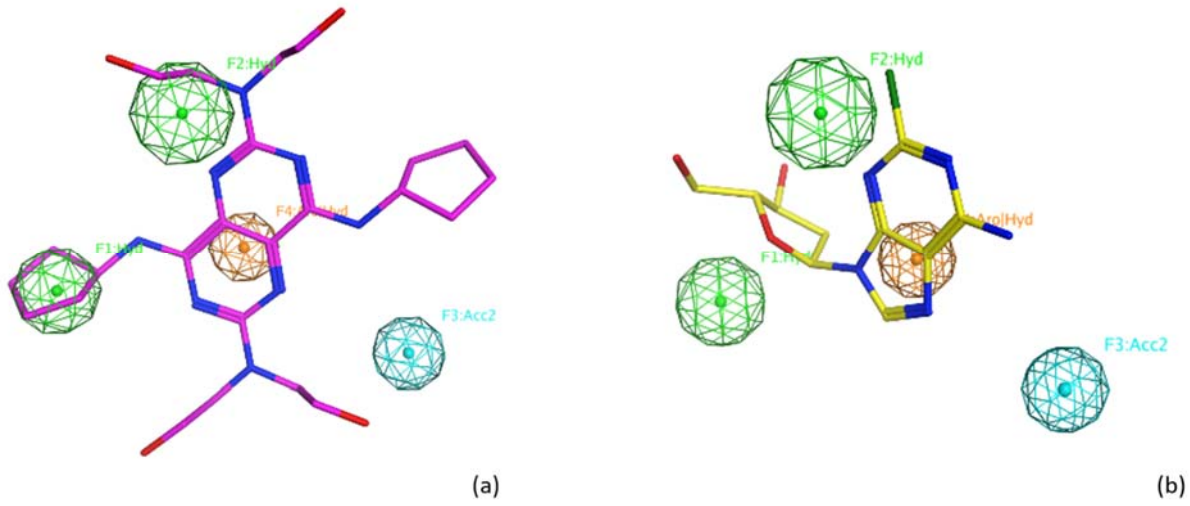

Figure 2. (a) hENT1 inhibitor aligned to PH4-36 fitting all pharmacophore features. (b) hENT1 permeants aligned to PH4-36 missing the two hydrophobic and acceptor projection features of the pharmacophore.

Figure 3a shows the overlay of the four training set inhibitors that resulted in generating query PH4-36 which exhibited the following features: (1) hydrophobic centroid feature with 1.2 in diameter; (2) hydrophobic centroid feature 1.4 in diameter; (3) Hydrogen bond acceptor projection and (4) aromatic or hydrophobic centroid feature (Figure 3b, 3c). Distance and angles between the features were shown in Figure 3d. For the other best performing inhibitor pharmacophore queries features listed in Table 2, see Supporting information Figure S1.

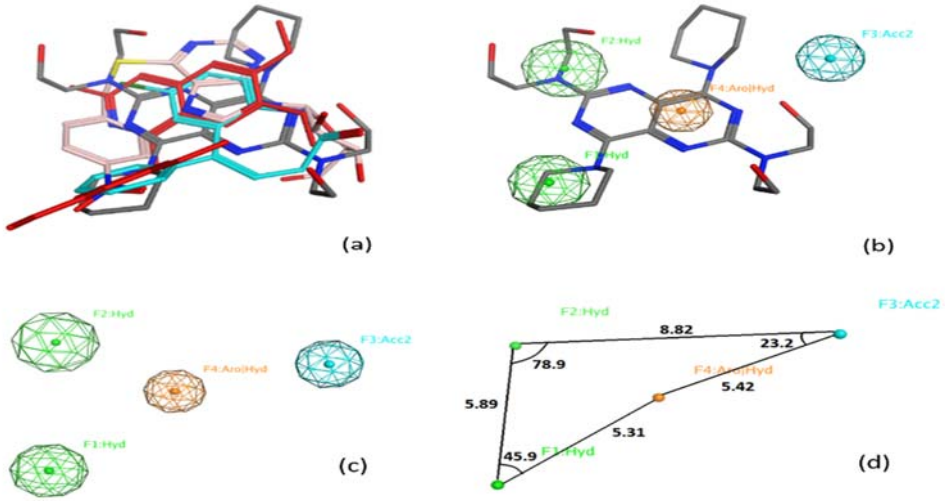

Figure 3. Pharmacophore query PH4-36 of the hENT1 inhibitors. (a) The inhibitors training set, consisting of 4 ligands, molecular superimposition. (b) An inhibitor molecule aligned with the pharmacophore query no. 36. (c) pharmacophoric features. (d) distances and angles between the pharmacophore features.

Similar to the PH4-36 features, prior research had shown that the best performing pharmacophoric features of ENT1 inhibitors were three hydrogen-bond acceptors, two aromatic rings, and a hydrophobic group generated by the PHASE modeling program using the potent ENT1 inhibitor NBTI and its two structurally related analogs.[30] Also, in partial agreement with our findings, Chen, et al. (2011) constructed a pharmacophore model that consisted of one aromatic ring and two hydrogen bond acceptors using the Catalyst program, based on one scaffold training set of structurally related 25 hENT1 inhibitors.[31]

Generally, some of the pharmacophoric features such as hydrogen bond acceptor and aromatic ring were common between our study and the studies mentioned above. However, the number of these pharmacophoric features differed among the studies. The variation in the number of features is due to the differences in the modeling program used and the different training compound sets utilized for pharmacophore model generation. It is also important to note that the previously mentioned studies had utilized a single scaffold in their relevant training sets.[30,31] On the other hand, we used four different scaffolds for pharmacophore generation, and hence PH4-36 shall be considered as a generalized pharmacophore that can help in discovering other new and novel scaffolds of hENT1 inhibitors.

For permeant pharmacophore generation, the training set consisted of two different scaffold molecules (Guanosine and Gemcitabine) (Supporting information Table S3, Figure S2) with low molecular weight, a low number of rotatable bonds and a high affinity to hENT1. The pharmacophore queries generated for hENT1 permeants consisted of four – five features (Table 3). A selectivity rate of 100% and a specificity rate of 84.62% was exhibited by PH4-23, which can be considered as the best performing and most discriminatory permeant pharmacophore (Table 3).

Figure 4a shows the superimposition of the two permeants Guanosine and Gemcitabine that resulted in generating PH4-23. Features of this pharmacophore were: one aromatic/planar system, two hydrogen bond donor projections and one hydrogen bond acceptor (Figure 4b, 4c). Distances and angles were calculated for PH4-23 (Figure 4d).

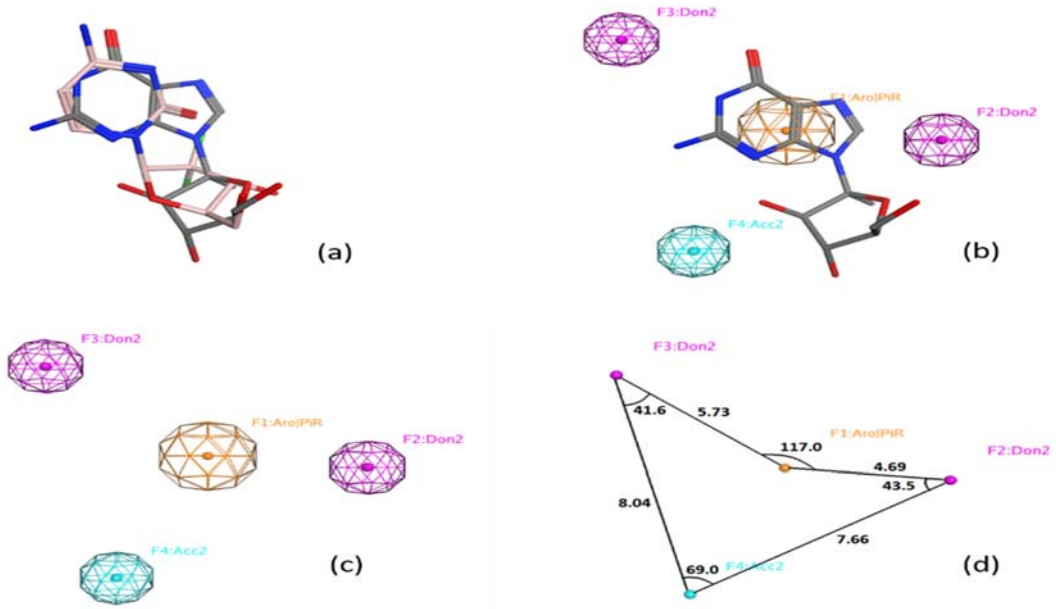

Figure 4. Pharmacophore query no. 23 of hENT1 permeants. (a) permeant's training set, consisting of 2 ligands Gemcitabine and Guanosine overlay. (b) A permeant molecule aligned with the pharmacophore query no. 23. (c) pharmacophoric features. (d) Distances and angles between pharmacophore features.

In terms of substrate structural requirement for ENT1 transport, substrate pentose sugars ribose/deoxyribose and arabinose moieties are primary determinates for transport.[1,6,32] Moreover, the substrate's pentose sugar C(3') hydroxyl group is essential for ENT1 binding.[1,32] Permeants such as nucleosides and nucleoside analog drugs are hydrophilic and, hence their permeation is presumed to be facilitated via pentose sugar C(3') hydroxyl group-hydrogen bonding interaction with ENT1. Similarly, the permeant pharmacophore PH4-23 did exhibit hydrogen bonding features.

3.4 Establishment of virtual screening using hENT1 inhibitor's pharmacophore

To examine the efficacy of the PH4-36 pharmacophore and its application in the drug design of new hENT1 inhibitors, we used this pharmacophore as a filter prior to a small-scale virtual screening (VS). The drug-like ligand library consisted of 5000 compounds; 56 were hENT1 inhibitors while the remaining compounds were the decoy set, obtained from a commercial ligand library (i.e., TimTec), all were filtered according to Lipinski's rule of five.[33] Then, the ligand library was docked into the crystal structure of hENT1 where the co-crystallized ligand was used for binding site identification purposes.

Three protocols were applied to the drug-like ligand library to screen virtually for the 56 hENT1 inhibitors (Scheme 1). These protocols were: SP, a standard docking-based VS with no filters; FP-1, a VS protocol preceded by the use of hENT1 inhibitor pharmacophore PH4-36 as filter-in. For the third protocol, FP-2, a further optimization step was added to the VS protocol by including a hENT1 permeants pharmacophore that filter-out permeants. Hence the third VS protocol, FP-2, was preceded by the use of the hENT1 permeants pharmacophore PH4-23 as filter-out, combined with hENT1 inhibitor pharmacophore PH4-36 as filter-in. Furthermore, to assess the screening protocol's success, the area under receiver operating characteristic (AU-ROC) curves were calculated. ROC graph is a

graphing method used for visualizing, evaluating and comparing the performance of the three VS protocols.[34,35] Each ROC curve depicts the correlation between the number of retrieved ligands of interest (true positive) and the number of decoys (true negative) at various portions of top-ranked ligands obtained from VS. The higher the value of AU-ROC, the better the performance of that screening protocol.

The initial glance of implementing the FP-1 protocol is that it immediately resulted in drastic downsizing for the 5000 ligands library by around 79% (i.e., down to 1034 compounds) relative to the SP protocol (Scheme 1). As for FP-2, the prepared ligand library was first passed through the permeant pharmacophore. The ligands that fit the permeant pharmacophore were excluded, while the remaining ones that did not fit were then passed through the second filter of the inhibitor pharmacophore. Similarly to FP-1, FP-2 resulted in a significant reduction of the 5000 ligand library down to 1031 compounds. FP-2 slightly downsized the ligand library to be docked onto the binding site (1013 compounds) compared to FP-1 (1034 compounds) (Scheme 1).

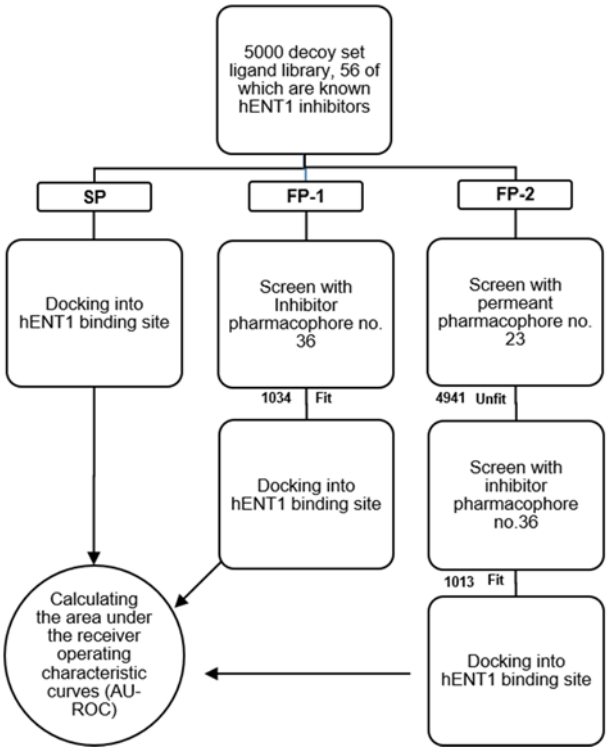

Scheme 1. The three virtual screening protocols utilized in the decoy set validation test.

We then determined the rate of retrieved inhibitors of the standard, one and two filtered-based protocols and performed a ROC analysis. In the top 1% of the 5000-docked ligands, retrieved rates of 19.6% and 21.3% were seen with the single-filter and dual-filter protocol, respectively, in comparison to the SP approach which showed less %EF of 12.5% (Table 4). Hence, the filter-based protocols were able to pull up a higher number of inhibitors at the top 1 % of the docked ligands compared to the non-filtered protocol. Similarly, the rate in the top 3% of the docked ligands was higher in the filter-based protocols with values of 35.3% in FP-1 and 34% in FP-2

than the standard non-filter approach which showed only 17.8% (Table 4). Remarkably, in the top 20% of docked ligands, while FP-1 and FP-2 were capable of retrieving almost all docked inhibitors (with %EF values of 98% and 100%, respectively), the SP approach was only capable of retrieving 57% of the hENT1 inhibitors (Table 4). Based on the rate of retrieved inhibitors (true positive rate) and the rate of retrieved decoys (true negative rate) at various portions of top-ranked ligands obtained from the three VS protocols, a ROC curves were plotted for the three protocols where AUC value for each curve was then calculated. AU-ROC values of 0.802, 0.927 and 0.941 were seen for SP, FP-1 and FP-2, respectively. The higher the AU-ROC value the better the performance is. Overall, the one and two filtered approaches consistently performed better, evident by the significantly higher AU-ROC value, relative to the non-filtered SP approach (Figure 5).

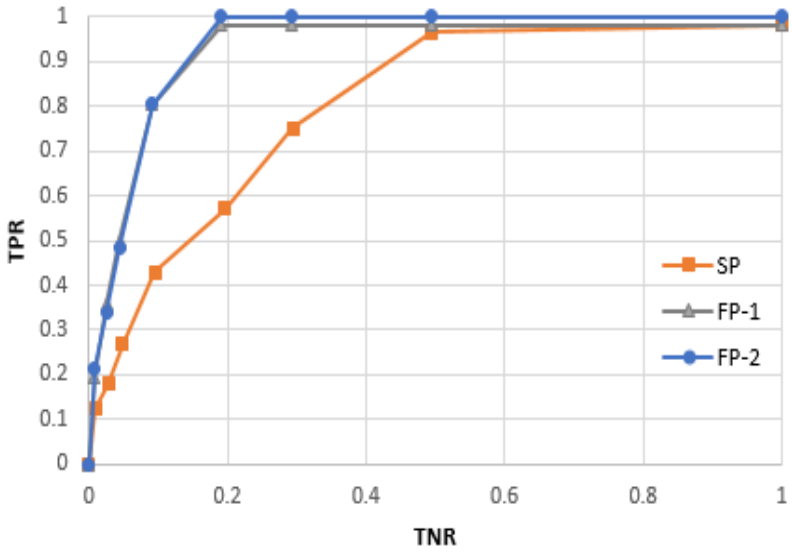

Figure 5. ROC analysis of the three assessed protocols: SP-1, non-filtered protocol; FP-1, one filter protocol; FP-2, two filters protocol. TPR: True Positive Rate; TNR: True Negative Rate.

Standard protocols for VS of a large-sized library have limitations; including the lengthy period of docking and scoring compounds, and the generation of many false-positive compounds that are ranked highly in docking scores ahead of the true positive compounds.[36] Similar to previous studies,[28,36,37] the VS results demonstrated the efficiency of the pharmacophore filter-based approach to pick up true hENT1 inhibitors over decoys, evident by the improved retrieval rates of the VS output compared with the nonfilter-based approach. Moreover, a significant reduction in the size of the ligand library was obtained by the filtered based approach to be docked on the hENT1 binding site, which resulted in the speed up of VS.

3.5 Analysis of inhibitors–hENT1 complexes

To identify the essential residues for inhibitors binding to hENT1, a PLIF was generated for the VS hENT1-docked inhibitors complexes using MOE software.[26] The PLIF-interaction occupancy of all interacting residues in the hENT1 binding site was then determined. The interaction occupancy is defined as the percentage of ligands interacting with the side or main chain of a given amino acid. A total of 20 residues were found to participate in the protein-ligand

interaction (Figure 6a). Trp29, Met33, Asn338, and Asp341 showed the highest binding interactions evident by their high % occupancies of ~ 45% in comparison to other residues (Figure 6b). Furthermore, hydrogen bonding and arene interaction with Met33; and hydrogen bonding with Trp29, Asn338, and Asp341 appeared to facilitate the inhibitors binding to hENT1 (Figure 6b).

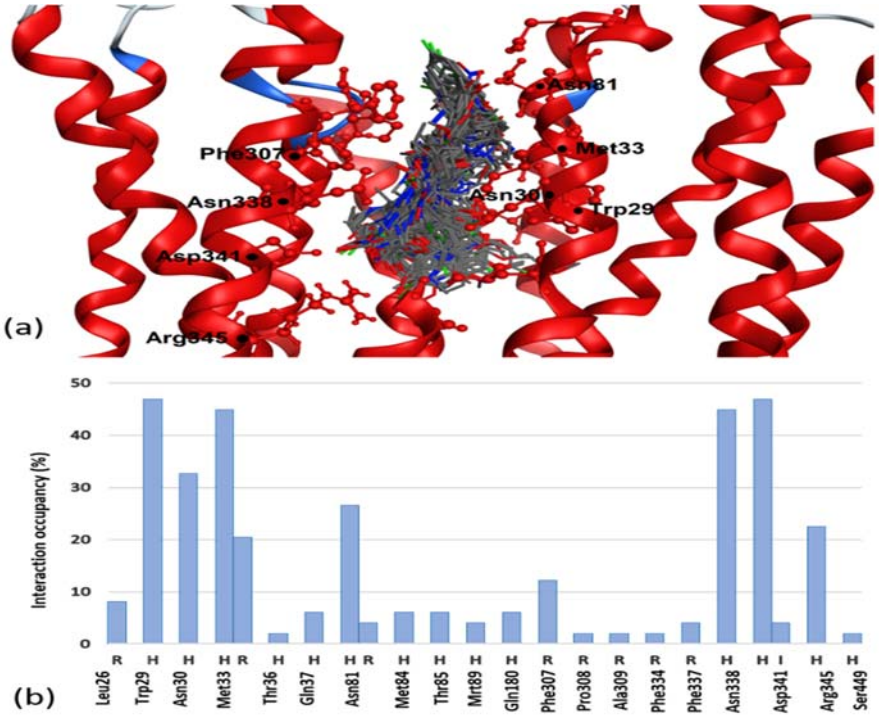

Figure 6. (a) The docked poses of inhibitors onto the crystal structure of the hENT1 α-helical TM domain. (b) Protein ligand interaction fingerprint of ENT1 inhibitors (H: H-bond attraction, I: ionic attraction, R: arene attraction).

Consistent with our structural findings, Trp29, Met33, and Asn338 have been previously shown to be necessary for the inhibitor Dilazep binding to hENT1.[8] Dilazep's trimethoxybenzoic acid group was shown to interact with Trp29, present within the orthosteric site of the hENT1 central cavity while the central diazepane ring of Dilazep interacted hydrophobically with Met33. In the hENT1 opportunistic site, located proximally to the orthosteric site, Dilazep's other trimethoxyphenyl ring formed hydrogen bonding with Asn338.[8] Similarly, we observed that arene interaction (possibly hydrophobic) with Met33 and hydrogen bonding with Asn338 facilitated the inhibitors interaction with hENT1 (Figure 6b). Asp341, another identified key residue that facilitated the inhibitors interaction with hENT1 in the current study, was reported to be essential for the binding of the inhibitor NBTI to hENT1. It was demonstrated that 3′-OH of the ribose moiety of NBTI interacted with Asp341 present within the hENT1 orthosteric site,[8] likely via hydrogen bonding. Overall, the results highlighted the key interaction residues for inhibitors binding to hENT1 and further confirms VS protocol's validity and applicability in selecting real hENT1 inhibitors given that the identified key interacting residues Trp29, Met33, Asn338, and Asp341, has been previously reported to be essential for inhibitors binding to hENT1.

4. CONCLUSION

In conclusion, we have reported the successful development of highly sensitive and selective pharmacophoric model for hENT1 inhibitors. Also, the present study demonstrated a new virtual screening protocol where the aforementioned inhibitor pharmacophore was used as filtration tools within the hENT1 inhibitors VS scheme. Furthermore, the proposed protocols were successfully able to reduce the size of the screened ligand library by almost 80% (prior to docking) and to accurately select the true hENT1 inhibitor among decoy ligands, which led to a more rapid and effective VS approach. The novel computer-aided protocol proposed in this work can help in the discovery of new hENT1 inhibitors as potentially acting cardio- and neuroprotective agents. Future studies will focus on utilizing the proposed virtual screening protocol to identify new prospective hENT1 inhibitors and testing their effect on hENT1 transport *in vitro* and *in vivo*.

ACKNOWLEDGEMENT

We would like to thank Dr. Arshad Mahmood for proofreading the manuscript.

TABLES

Table 1. Mean values (±standard deviations) of calculated physicochemical parameters for inhibitors.

Physicochemical property	Inhibitors (± SD)	Permeants (± SD)
Mean MWT [a](Da)	473.52 ± 136.24	269.70 ± 34.36
Mean #HBA [b]	4.82 ± 2.35	6.05 ± 1.51
Mean #HBD [c]	2 ± 1.82	3.72 ± 1.13
Mean Log P	1.87 ± 2.08	-1.56 ± 0.65
Mean No. of rotatable bonds	10 ± 6.13	2.22 ± 0.65
Mean PSA [d] (Å2)	180.8 ± 88.7	37.01 ± 86.31
Mean HSA [e] (Å2)	708.63 ± 117.32	423.79 ± 89.54

[a] Molecular Weight; [b] Number of Hydrogen Bond Acceptor, [c] Number of Hydrogen Bond Donor, [d] Polar Surface Area, [e] Hydrophobic Surface Area.

Table 2. The selectivity and specificity of the best performing pharmacophore for inhibitors

PH4 no.	**Features**	**Selectivity 'Se' (%)**	**Specificity 'Sp' (%)**
1	1: Hyd 2: Acc2 3: Acc 4; Aro | Hyd	92.30	75
4	1:Hyd 2:Acc2 3:Aro|Hyd 4:Don|Acc	94.23	43.75
6	1:Hyd 2:Hyd 3:Acc2 4:Aro|Hyd	82.69	81.25
21	1:Hyd 2:Acc2 3:Aro|Hyd 4:Acc|Cat	86.53	75.00
30	1:Hyd 2:Hyd 3:Acc2 4:Acc	92.30	62.5
36	**1:Hyd 2:Hyd 3:Acc2 4:Aro|Hyd**	**92.30**	**87.5**
40	1:Hyd 2:Aro|Hyd 3:Aro|Hyd 4:Don|Acc	88.5	100

Aro: Aromatic center, Don: H-bond donor, Hyd: hydrophobic centroid, Acc: H-bond acceptor, Acc2: H-bond acceptor projection, Cat: cationic

Table 3. The selectivity and specificity of the best performing pharmacophore for hENT 1 permeants.

PH4 no.	Features	Selectivity Se (%)	Specificity Sp (%)
8	1:Don2 2:Acc2 3:Aro|Hyd 4:Don|Acc 5:Acc|Cat	93.75	69.23
9	1:Aro|PiR 2:Hyd 3:Don 4:Acc 5:Aro|Hyd	87.5	82.69
16	1:Aro|PiR 2:Hyd 3:Acc2 4:Don	100	75
17	1:Aro|PiR 2:Hyd 3:Acc2 4:Don|Ani	100	75
21	1:Aro|Hyd 2:Don|Acc 3:Don|Acc 4:Don|Acc 5:Acc|Cat	100	65.38
23	**1:Aro|PiR 2:Don2 3:Don2 4:Acc2**	**100**	**84.62**
28	1:Aro|PiR 2:Acc2 3:Acc 4:Aro|Hyd	93.75	61.54
49	1:Don2 2:Aro|Hyd 3:Don|Acc 4:Don|Acc 5:Acc|Cat	93.75	75

Aro: Aromatic center, Don: H-bond donor, Hyd: hydrophobic centroid, Acc: H-bond acceptor, Acc2: H-bond acceptor projection, Don2: H-bond donor projection, Cat: Cationic, PiR: Pi ring or Aromatic

Table 4. Retrieved rate of hENT1 inhibitors at various portions of the sorted docked ligands from filter-based and non-filtered-based VS.

Output percentage of the top-ranked docked 5000-ligand library	The rate of retrieved inhibitors		
	No-filter	One filter	Two filters
1	12.5	19.6	21.27
3	17.8	35.29	34.04
5	26.78	49.02	48.93
10	42.85	80.39	80.85
20	57.14	98.04	100

REFERENCES

.1 Boswell-Casteel RC, Hays FA. Equilibrative nucleoside transporters-A review. Nucleosides Nucleotides Nucleic Acids 2017; 36(1): 7-30.

.2 King AE, Ackley MA, Cass CE, Young JD, Baldwin SA. Nucleoside transporters: from scavengers to novel therapeutic targets. Trends Pharmacol Sci 2006; 27(8): 416-25.

.3 Pastor-Anglada M, Perez-Torras S. Who Is Who in Adenosine Transport. Front Pharmacol 2018; 9: 627.

.4 Pastor-Anglada M, Perez-Torras S. Nucleoside transporter proteins as biomarkers of drug responsiveness and drug targets. Front Pharmacol 2015; 6: 13.

.5 Baldwin SA, Beal PR, Yao SY, King AE, Cass CE, Young JD. The equilibrative nucleoside transporter family, SLC29. Pflugers Arch 2004; 447(5): 735-43.

.6 Huang W, Zeng X, Shi Y, Liu M. Functional characterization of human equilibrative nucleoside transporter 1. Protein Cell 2017; 8(4): 284-95.

.7 Sundaram M, Yao SY, Ingram JC, et al. Topology of a human equilibrative, nitrobenzylthioinosine (NBMPR)-sensitive nucleoside transporter (hENT1) implicated in the cellular uptake of adenosine and anti-cancer drugs. J Biol Chem 2001; 276(48): 45270-5.

.8 Wright NJ, Lee SY. Structures of human ENT1 in complex with adenosine reuptake inhibitors. Nat Struct

Mol Biol 2019; 26(7): 599-606.

.9 Abd-Elfattah AS, Jessen ME, Lekven J, Wechsler AS. Differential cardioprotection with selective inhibitors of adenosine metabolism and transport: role of purine release in ischemic and reperfusion injury. Mol Cell Biochem 1998; 180(1-2): 179-91.

.10 Figueredo VM, Diamond I, Zhou HZ, Camacho SA. Chronic dipyridamole therapy produces sustained protection against cardiac ischemia-reperfusion injury. Am J Physiol 1999; 277(5): H2091-7.

.11 Rose JB, Naydenova Z, Bang A, et al. Equilibrative nucleoside transporter 1 plays an essential role in cardioprotection. Am J Physiol Heart Circ Physiol 2010; 298(3): H771-7.

.12 Zhu Z, Hofmann PA, Buolamwini JK. Cardioprotective effects of novel tetrahydroisoquinoline analogs of nitrobenzylmercaptopurine riboside in an isolated perfused rat heart model of acute myocardial infarction. Am J Physiol Heart Circ Physiol 2007; 292(6): H2921-6.

.13 Effendi WI, Nagano T, Kobayashi K, Nishimura Y. Focusing on Adenosine Receptors as a Potential Targeted Therapy in Human Diseases. Cells 2020; 9(3.(

.14 Guitart X, Bonaventura J, Rea W, et al. Equilibrative nucleoside transporter ENT1 as a biomarker of Huntington disease. Neurobiol Dis 2016; 96: 47-53.

.15 Kao YH, Lin MS, Chen CM, et al. Targeting ENT1 and adenosine tone for the treatment of Huntington's disease. Hum Mol Genet 2017; 26(3): 467-78.

.16 Huang NK, Lin JH, Lin JT, et al. A new drug design targeting the adenosinergic system for Huntington's disease. PLoS One 2011; 6(6): e20934.

.17 Noji T, Karasawa A, Kusaka H. Adenosine uptake inhibitors. Eur J Pharmacol 2004; 495(1): 1-16.

.18 Choi JS, Berdis AJ. Nucleoside transporters: biological insights and therapeutic applications. Future Med Chem 2012; 4(11): 1461-78.

.19 Tromp RA, Spanjersberg RF, von Frijtag Drabbe Kunzel JK, AP IJ. Inhibition of nucleoside transport proteins by C8-alkylamine-substituted purines. J Med Chem 2005; 48(1): 321-9.

.20 Williams C. Reverse fingerprinting, similarity searching by group fusion and fingerprint bit importance. Mol Divers 2006; 10(3): 311-32.

.21 Prieto-Martínez FD, Arciniega, M., & Medina-Franco, J. L. . Molecular docking: current advances and challenges. TIP Revista especializada en ciencias químico-biológicas 2018; 21.

.22 MOE. Molecular Operating Environment, Chemical Computing Group, http://wwwchemcompcom, Montreal, Canada 2019.

.23 Schrödinger. Glide, LLC, New York, NY, 2020 2020.

.24 Friesner RA, Murphy RB, Repasky MP, et al. Extra precision glide: docking and scoring incorporating a model of hydrophobic enclosure for protein-ligand complexes. J Med Chem 2006; 49(21): 6177-96.

.25 Ghattas MA, Atatreh N, Bichenkova EV, Bryce RA. Protein tyrosine phosphatases: Ligand interaction analysis and optimisation of virtual screening. J Mol Graph Model 2014; 52: 114-23.

.26 ULC CCG. Molecular Operating Environment, (MOE) 2016.

.27 Labute P. A widely applicable set of descriptors. J Mol Graph Model 2000; 18(4-5): 464-77.

.28 Al Rawashdah S, Hamrouni A, Sadek B, et al. Molecular modelling studies on a7 nicotinic receptor allosteric modulators yields novel filter-based virtual screening protocol. J Mol Graph Model 2019; 92: 44-54.

.29 Maruca A, Ambrosio FA, Lupia A, et al. Computer-based techniques for lead identification and optimization I: Basics. Physical Sciences Reviews 2019; 4(6.(

.30 Zhu Z, Buolamwini JK. Constrained NBMPR analogue synthesis, pharmacophore mapping and 3D-QSAR modeling of equilibrative nucleoside transporter 1 (ENT1) inhibitory activity. Bioorg Med Chem 2008; 16(7): 3848-65.

.31 Chen JB, Liu EM, Chern TR, et al. Design and synthesis of novel dual-action compounds targeting the adenosine A(2A) receptor and adenosine transporter for

neuroprotection. ChemMedChem 2011; 6(8): 1390-400.

.32 Rehan S, Shahid S, Salminen TA, Jaakola VP, Paavilainen VO. Current Progress on Equilibrative Nucleoside Transporter Function and Inhibitor Design. SLAS Discov 2019; 24(10): 953-68.

.33 Lipinski CA, Lombardo F, Dominy BW, Feeney PJ. Experimental and computational approaches to estimate solubility and permeability in drug discovery and development settings. Adv Drug Deliv Rev 2001; 46(1-3): 3-26.

.34 Fawcett T. An introduction to ROC analysis. Pattern Recognition Letters 2006; 27(8): 861-74.

.35 Hevener KE, Zhao W, Ball DM, et al. Validation of molecular docking programs for virtual screening against dihydropteroate synthase. J Chem Inf Model 2009; 49(2): 444-60.

.36 Suaifan GARY, Al-Ejal HAN, Taha MO. Pharmacophore and QSAR modeling of endothelial nitric oxide synthase inhibitors and subsequent validation and in silico search for new hits. Jordan Journal of Pharmaceutical Sciences 2012; 5 (3): 220-42.

.37 Peach ML, Nicklaus MC. Combining docking with pharmacophore filtering for improved virtual screening. J Cheminform 2009; 1(1): 6.

.38 Atatreh N, Ghattas MA, Bardaweel SK, Rawashdeh SA, Sorkhy MA. Identification of new inhibitors of Mdm2-p53 interaction via pharmacophore and structure-based virtual screening. Drug Des Devel Ther 2018; 12: 3741-52.

39. Al-Shar'i NA, Hassan M, Al-Balas Q, Almaaytah A. Identification of Possible Glyoxalase II Inhibitors as Anticancer Agents by a Customized 3D Structure-Based Pharmacophore Model. Jordan Journal of Pharmaceutical Sciences 2015; 8: 83-103.

تطوير فارماكوفور جديد لاستخدامه كمرشح نوعي خلال عملية اكتشاف مركبات مثبطة لناقلات النوكليوزيدات البشرية المتوازنة

عزة رمضان[1*]، شيماء حسن[1*]، سيدرا جمال[1*]، إسماعيل مؤمن[1*]، نور عطاطرة[1*]، محمد غطاس[1*]

1 كلية الصيدلة، جامعة العين، أبوظبي، الإمارات العربية المتحدة

*قدم هؤلاء المؤلفين مساهمات متساوية، يتشاركون في الباحث الأول

ملخص

تعتبر ناقلات النيوكليوسيدات البشرية المتوازنة **(hENTs)** بروتينات مهمة تسمح للنيوكليوسيدات والقواعد النيتروجينيه بالنفاذ إلى الخلية. يعتبر **HENT 1** هدفًا واعدًا ضد أمراض القلب وأمراض هنتنغتون حيث أن تثبيطه يترتب عليه تأثيرات علاجية محتملة مثل الحماية من بعض أمراض القلب والأعصاب. ومع ذلك، فإن مثبطات **hENT1** المتعارف عليها حاليا لها خصائص دوائية ضعيف، بالتالي بحاجة إلى تطوير مثبطات جديدة. لذلك، قمنا بتطوير بروتوكول حاسوبي له القدرة على تمييز وانتقاء مثبطات **hENT1** بطريقة فعالة ومحددة. أولاً، تم إنشاء عدد من فارماكوفور (حامل الخصائص الدوائية) باستخدام مجموعة من المثبطات المعروفة مسبقا. ومن المثير للاهتمام، أن أفضل فارماكوفور للمثبطات قد أظهر معدلات انتقائية وخصوصيه عالية بلغت **92**٪ و**88**٪ على التوالي. إضافة الى ذلك، أدى استخدام مثبط فارماكوفور كمرشح إلى تحسين نتائج الغربلة الافتراضي القائمة على تقنية **docking** الى ما يقارب الضعف. يمكن أن يكون هذا النهج في تطبيق المحاكاة الحاسوبية **(in silico)** مفيدًا جدًا في تطوير مثبطات **hENT1** جديدة.

الكلمات الدالة: تصميم الدوائي ، ناقلات النيوكليوسيدات البشرية المتوازنة 1، المثبط، حامل الخصائص الدوائية.

تاريخ استلام البحث 2021/1/19 وتاريخ قبوله للنشر 2021/6/6.